Journal of GeoEngineering, Vol. 14, No. 1, pp. 11-20, March 2019
http://dx.doi.org/10.6310/jog.201903_14(1).2

PARAMETRIC ASSESSMENT OF LATERAL PRESSURE ON PILES AND LAGGINGS IN AN ANCHORAGE SYSTEM

Hajar Gharedaghi [1] and Hadi Shahir [2*]

ABSTRACT

Due to the difference of stiffness between laggings and piles in anchored soldier pile walls, soil arching usually occurs between piles. This causes non-uniform distribution of soil pressure and pressure concentration behind soldier piles. In the existing empirical diagrams for the lateral earth pressure on braced and anchored walls; which are based on the measurement of the created forces in strut elements so called "apparent pressure diagram"; the simultaneous impact of friction angle, soil cohesion, and surcharge effects has not been considered. In addition, the diagrams provide no information on the pressure on laggings. To answer these questions, the distribution of soil pressure in an anchored soldiered wall was studied using 3D numerical modeling. Variable parameters in the modeling include soil parameters, height of wall, horizontal distance of soldier piles, and surcharge. Results of parametric analysis show that the pressure applied on the anchored wall exceeded the values presented in the apparent pressure diagrams. Moreover, the surcharge-induced earth pressure, which is classically applied with active lateral pressure coefficient in equations, is greater, and it is about 70% more than that.

Key words: Anchor, soldier pile, lagging, soil pressure, arching, surcharge.

1. INTRODUCTION

A failing soil mass tends to exert pressure into its adjacent rigid borders. The phenomenon of soil mass pressure exertion into a harder element is called "arching". In fact, arching phenomenon causes a non-uniform distribution of stress. The arching phenomenon was first introduced by Terzaghi (1943) using trap door analogy. In retaining walls, soil arching allows structural elements of wall facing to be executed discontinuously. In an anchorage system, the stiffness difference between soldier piles and laggings cause the pressure to move to more rigid elements; therefore, the laggings play a minor role in bearing pressure on the wall.

The study of pressure on a retaining wall is a major issue in geotechnical engineering. Coulomb (1776) achieved the pressure on a retaining wall based on the limit equilibrium method; of course, lateral stress distribution is not clear in his method. Based on the laboratory studies conducted by Tsagareli (1965) and Fang and Ishibashi (1986), pressure distribution on a rigid retaining wall is non-linear. The analytical studies indicate that the non-linearity of soil pressure distribution is due to soil arching phenomenon (Handy 1985; Harrop-Williams 1989; Paik and Salgado 2003; Goel and Patra 2008). The research results indicate that the effect of soil arching on the horizontal stresses on a wall should be considered for the realistic estimation of the amount and distribution of soil pressure in a retaining wall design.

In the anchored soldier pile walls in which construction sequences are top to bottom, it is not accurate to use the equation proposed by Coulomb. Several factors such as wall height and specifications of soil, wall facing, and anchors affect wall displacement and consequently the pressure on the wall. Due to the complexity of pressure distribution and multiplicity of the factors affecting stress on wall in an anchorage system, the diagrams of apparent earth pressure can be used. Two of the most famous graphs in this field are the pressure distribution proposed by Terzaghi and Peck (1967) and Tschebotarioff (1951). They proposed some graphs for sandy and clayey soils separately; however, the c-ϕ soil were not examined. The diagrams did not show the effect of surcharge on the pressure imposed on the wall. Another drawback of the graphs is that they fail to specify part of the pressure borne by laggings.

Few studies have been conducted in this field including the numerical modeling of Vermeer *et al*. (2001), which discussed the effect of arching on the pressure distribution in a soldier pile wall. They examined pressure distribution using Plaxis3D with respect to Mohr-Coulomb and hardening constitutive models. The results indicate the concentration of stress is evident behind the soldier piles. In fact, horizontal stresses between the piles reduces and reaches zero. Hosseinian and Seifabad (2013) studied the effect of soldier piles distance on the arching. Their study indicates that changing the distance of piles is effective in lateral stress distribution. In fact, the force on the pile reduced with the distance between the piles increasing.

The analytical relation proposed by Spencer *et al.* (1986) can be referred to on the pressure imposed on lagging, which discussed horizontal arching phenomenon based on the theory proposed by Terzaghi (1943). The equation proposed by Spencer *et al*. (1986) shows the maximum pressure on lagging elements with respect to angle of friction, soil cohesion, and distance between soldier piles. The pressure distribution obtained from their proposed relation is uniform throughout the depth of wall. Some studies were conducted on lagging elements in recent years including the studies carried out by Perko and Boulden (2008), Cheng-Fang *et al*. (2011), and Bing-Xiong *et al.* (2013). Perko and Boulden (2008) achieved an equation for calculating the

Manuscript received April 13, 2018; revised August 13, 2018; accepted August 23, 2018.
[1] Master, Department of Civil Engineering, Faculty of Engineering, Kharazmi University, Tehran, Iran.
[2*] Assistant Professor (corresponding author), Department of Civil Engineering, Faculty of Engineering, Kharazmi University, Tehran, Iran (e-mail: shahir@khu.ac.ir).

pressure on lagging using analytical relations. The relation considered friction angle, the distance between piles, and surcharge. Pressure distribution is non-linear up to reaching the maximum pressure and it is uniform along the wall height. Bing-Xiong *et al.* (2013) proposed an analytical relation on the pressure imposed on lagging with respect to the effect of soil friction angle and the distance between piles. The relations show no concurrent effects of soil cohesion and surcharge parameters. In all the relations, the pressure on lagging is independent from the wall height; however, as proposed by FHWA anchorage manual, lagging thickness is considered variable for the walls with varied heights.

This article discussed the effect of various parameters on the pressure applied on soldier pile and lagging using 3D finite elements modeling in Plaxis 3D Foundation. Briaud and Lim (1999) article was used for validating the numerical model. Two types of c-ϕ soils with varied specifications were used in the parametric analysis. The analyses are for the walls with the heights of 12 and 24 m, the horizontal distances of 2, 3, and 4 m between the piles, and the surcharges of 50, 100, and 150 kPa. Finally, some relations are proposed on the pressure applied on the soldier pile and lagging.

2. METHOD OF NUMERICAL MODELING AND VERIFICATION

Modeling was performed in Plaxis 3D Foundation finite element software. The elements used in Plaxis include soil, pile, horizontal and vertical beams, wall, and spring. A beam element with linear elastic behavior was used for simulating pile behavior. The parameters of beam element include Young's modulus (E), the Poisson coefficient (υ), and the moment of inertia. Wall element is used for lagging modeling. d is the wall thickness and γ is the density. Wall stiffness includes modulus of elasticity and shear modulus (G). In the behavioral model of hardening soil, the secant modulus at 50% strength (E_{50}), unloading-reloading stiffness (E_{ur}), oedometric loading tangential stiffness (E_{oed}), and the parameters related to Mohr-Coulomb model (ϕ, c, and ψ). "Very fine" size was used for meshing. Structural elements (beams, floors, and walls) have rotational degrees of freedom (φ_x, φ_y, φ_z) in addition to the translational degrees of freedom (u_x, u_y, u_z). When such elements are connected (*i.e.*, when they share at least one geometry point), they will use the same degrees of freedom in these connection points. This applies to the translational degrees of freedom as well as the rotational degrees of freedom. As a result, the connection between these elements is rigid (moment connection). When floors or beams are connected to walls, the node pairs of the interface element adjacent to the wall are locally 'degenerated' to a single node to avoid a disconnection between the wall and the floor or beam.

Plaxis 3D Foundation is unable to model an inclined anchor element. Therefore, in this research a spring element was used for anchor modeling. The spring element should have been able to model free length and anchor prestressing specifications. In fact, anchor acts as a spring in which a considerable deformation do not occurs before the anchor force reaches prestressing force. However, deformation occurs in anchor after anchor force reaches prestressing force. With respect to the modeling limitations, anchor pretesting is considered as a concentrated load and anchor free length was used for spring stiffness ($K = EA/L_{ub}$). In this equation, E is the elastic modulus of anchor, A is the anchor's cross section area, and L_{ub} is the unbonded length of the anchor. There is a proper agreement between the results of model analysis and the results of Plaxis 2D models, which indicates appropriate assumptions of the anchor modeling in 3D. Due to the nearly plane strain condition of the wall, the general behavior and overall deformation of the wall were expected to be similar in the 2D and 3D simulations. So, by comparing 2D and 3D modeling results, the validity of the anchor modeling assumptions was assessed.

The information in Briaud and Lim (1999) was used to verify the numerical model. The study model consists of an anchored soldier pile wall with a maximum height of 7.5 m and length of 50 m. The centre-to-centre distance of piles is 2.44 m, which have been retained using two rows of anchors as shown by Fig. 1. The wall was instrumented with vibrating wire strain gauges on the soldier piles to obtain bending moment profiles, with inclinometer casings to obtain horizontal deflection profiles, and with load cells at the anchor heads to monitor the anchor forces. The location of inclinometers was shown in Fig. 1. It is a sandstone type of soil with the friction angle of 32°, the density of 18.5 kN/m^3, and a modulus of elasticity of 30 MPa. Pile cross section is HP 6 × 24 with a buried depth of 1.65 m. The height and thickness of the laggings were 30 and 7.5 cm, respectively. The anchors have an angle of 30° with the horizon. The total length and bonded length of the anchors are 12.35 m and 7.3 m, respectively. The diameter of reinforcing element is 25 mm. The prestressing forces of the anchor on the first and the second rows are 182.35 and 160 kN, respectively. Tables 1 to 3 show respectively the material specifications including soils, wall, and pile.

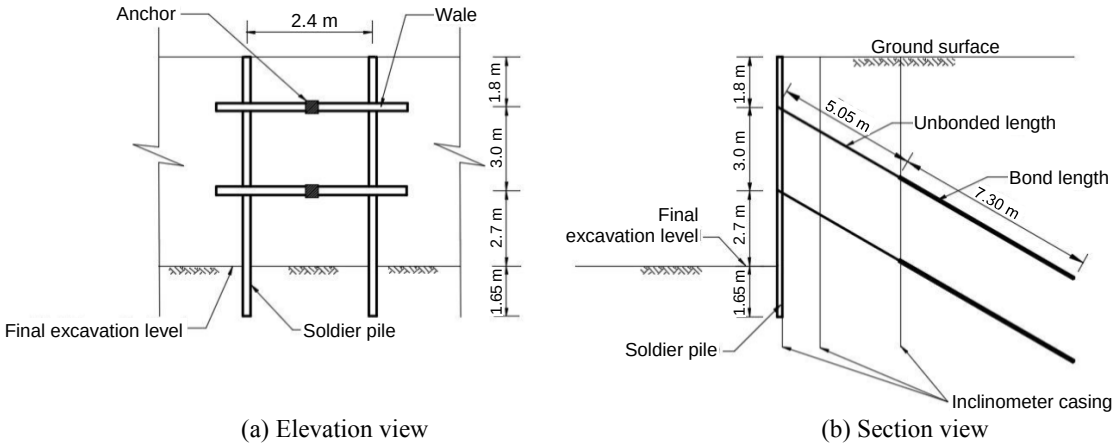

(a) Elevation view (b) Section view

Fig. 1 Specifications of the anchored wall (Briaud and Lim 1999)

Table 1 Soil specification used in the verification model (Briaud and Lim 1999)

Parameter	Symbol	Unit	Value
Unit weight	γ	kN/m^3	18.5
Elastic modulus	E	kPa	2.5×10^4
Friction angle	ϕ	deg	32
Cohesion	c	kPa	0
Dilatancy angle	ψ	deg	2

Table 2 Wall specification used in the verification model (Briaud and Lim 1999)

Parameter	Symbol	Unit	Value
Thickness	d	mm	100
Elastic modulus	E	kPa	1.365×10^6

Table 3 Pile specification used in the verification model (Briaud and Lim 1999)

Parameter	Symbol	Unit	Value
Diameter	D	m	0.25
Area	A	m^2	0.011
Moment of inertia against bending around the second axis	I_2	m^4	5.5×10^{-5}
Moment of inertia against bending around the third axis	I_3	m^4	5.5×10^{-5}

The main features of Briaud and Lim (1999) simulation are similar to the current study. The initial shape of the mesh was rectangular, which was 76 m in length, 16.5 m in height, and 2.44 m in width. The first step was to turn the gravity stresses. The second step was to install the piles; this consisted of activating the beam elements and allowing them to be stressed by the next steps. Therefore, driving stresses were not simulated. The third step was to excavate the first lift. This step induced initial deflections and a change in stress. The fourth step was to install the wood lagging and the first row of anchors. This step consisted of activating the shell elements simulating the wood lagging and activating the beam elements simulating the tendon bonded length of the anchor. The sixth step consisted of activating the spring element simulating the unbonded tendon length. The seventh step was the excavation of the next lift.

To define construction steps, only boundaries and soil mass are activated in the first phase of calculations. Pile element is activated in the second phase with respect to the buried depth on the ground. Displacement is changed into zero in both the first and the second phases. In the following steps, construction steps including excavation, anchor installation, and lagging installation are applied, respectively.

The modeling results have been compared with the values measured in the field and the modeling results achieved by Briaud and Lim (1999) using Abaqus (Fig. 2). The comparison indicates that the value predicted for displacement of the top of the wall is consistent with the measured value properly. Of course, the deformation of wall height in the finite elements analysis is almost uniform; however, lower values are seen at lower levels in the measured values. The trend of deformation changes in the wall height in the modeling carried out by Briaud and Lim (1999) and it is almost similar to the results achieved in the present modeling. The changes of bending moment in the wall height are appropriately consistent and the changes of bending moment have been predicted properly. The axial force values, except in surface depths, are consistent appropriately with the measured values in other depths; however, the finite elements results achieved by Briaud and Lim (1999) predicted greater values for the axial force of pile. Consequently, the numerical model used in this research is capable of predicting different components of the anchored soldier pile wall performance.

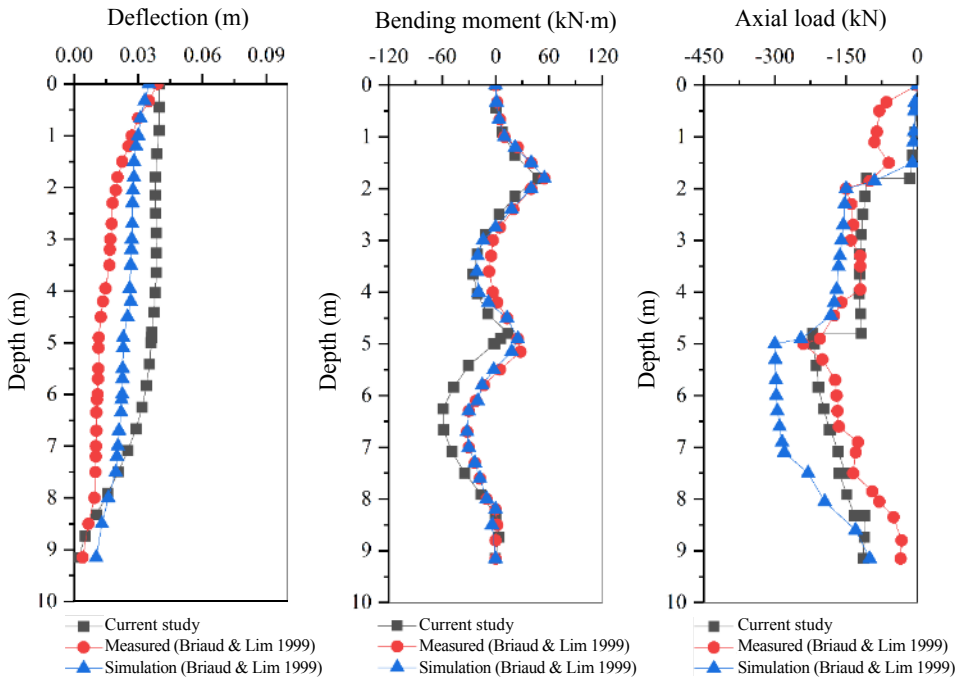

Fig. 2 Comparison of results of current study, measured values, and Briaud and Lim (1999)

3. PARAMETRIC ANALYSIS

Numerical models were analysed with respect to different parameters to obtain the pressure of soil on the pile and lagging. This study examined the parameters such as wall height, horizontal distance between piles, type of soil, and surcharge. Excavation was considered at the two heights of 12 and 24 m and the horizontal distances between the piles were considered at 2, 3, and 4 m. The soil profile contains one layer of soil. Two types of c-ϕ soil were considered in this study. Soil type 1 is indicated a cemented gravelly soil and soil type 2 is a lightly cemented (or clayey) sandy soil. The soil model used in the simulation, is the hardening soil model. the hardening-soil model is an advanced model for the simulation of soil behavior. As for the Mohr-Coulomb model, limiting states of stress is described by means of the friction angle, ϕ, the cohesion, *c*, and the dilatancy angle, ψ. However, soil stiffness is described much more accurately by using three different input stiffness: the triaxial loading stiffness, E_{50}, the triaxial unloading stiffness, E_{ur}, and the oedometer loading stiffness, E_{oed}. As average values for various soil types, $E_{ur} \approx 4\ E_{50}$ and $E_{oed} \approx E_{50}$. Table 4 examines two types of soils with varied specifications. The pile sections were considered in such a way that they were sufficient for the most critical situation in each wall height. For the walls with the heights of 12 and 24 m, 2IPE300 and 2IPE360 were respectively used and Table 5 shows the used specifications. For the walls with the heights of 12 and 24 m, lagging element thicknesses of 150 and 200 mm were respectively considered, and Table 6 shows the wall specifications. The layout of anchors is uniform on the wall surface and their horizontal and vertical distances were considered equal ($S_H = S_V$). As shown by Fig. 3, the horizontal distance of anchoring elements and the horizontal distances of piles (S_H) are equal. The distance between the ground level and the first anchor and between the last anchor and the foundation bottom is $S_v/2$.

Table 4 Soil specifications used in the parametric analysis

Parameter	Symbol	Unit	Value	
			Soil type 1	Soil type 2
Unit weight	γ	kN/m^3	20	19
Elastic modulus	*E*	MPa	80	30
Friction angle	ϕ	deg.	36	32
Cohesion	*c*	kPa	30	10
Dilatancy angle	ψ	deg.	6	2

Table 5 Pile specifications used in the parametric analysis

Parameter	Symbol	Unit	Value	
			2IPE300	2IPE360
Area	*A*	m^2	0.011	0.015
Moment of inertia against bending around the second axis	I_2	m^4	7.03×10^{-5}	1.22×10^{-4}
Moment of inertia against bending around the third axis	I_3	m^4	3.29×10^{-4}	1.7×10^{-4}

Table 6 Wall specifications used in the parametric analysis

Parameter	Symbol	Unit	Value	
Thickness	*d*	mm	150	200
Unit wright	γ	kN/m^3	9	9
Elastic modulus	*E*	kPa	1.5×10^6	1.5×10^6

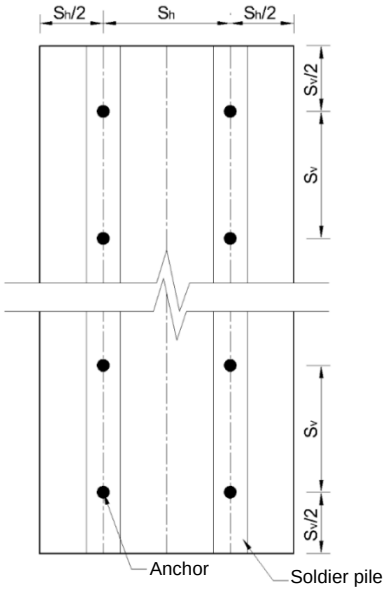

Fig. 3 Wall facing geometry for parametric analysis

The specifications of the anchors and their prestressing force in any model have been considered uniformly in the whole wall height and limit analysis method has been used to determine them. The method proposed in the design using limit equilibrium method based on FHWA-IF-99-015 manual is to apply a uniform force equal to the whole force of anchors on wall facing. Based on the items stated in FHWA-IF-99-015, the values obtained from limit equilibrium method in coarse-aggregate soils are equal to the apparent pressure method if the safety factor of 1.3 is used in stability analysis. Therefore, the uniform force applied on the wall in this study is equal to the total prestressing force of anchors in surface unit with respect to the safety factor of 1.3. By applying the parameters effective in modeling and determining the range and values of each for the analysis, anchor design is performed in Slope/W. The analysis provides the specifications such as anchor length, unbonded length, anchor inclination, cross section area, and the prestressing force. The force on the wall surface unit depends on soil type, wall height, and surcharge. However, the results indicate the independency of prestressing force in surface unit on the distance of anchors. After making the calculations, the values for prestressing of anchors in surface unit are shown by Table 7 for different types of soils, wall heights, and surcharges. As the table shows, for any identical amount of surcharge, type of soil, and wall height, regardless of the distances between anchors, the force imposed on anchors in surface unit is equal. The prestressing force of each anchor is achieved by Eq. (1) using the Table 7. In this equation, *P* is the required prestressing in surface unit and S_H and S_V are respectively the horizontal and vertical distances between anchors.

Table 7 Anchors prestress force in the unit area of wall facing

Unit: kPa

Soil type		Type 1		Type 2		Type 1 without cohesion		Type 2 without cohesion	
Wall height (m)		12	24	12	24	12	24	12	24
Surcharge (kPa)	0	2	60	27.5	90	32	90	37.5	100
	50	20	80	50	115	52	110	60	125
	100	40	100	72.5	140	–	–	–	–
	150	60	120	95	165	–	–	–	–

$$T = P \times S_H \times S_V \quad (1)$$

Modeling is performed in Plaxis 3D after specifying the prestressing force and the specification of anchors. The inclination of all anchors is 15° and the unbonded length of anchors is considered as large as the biggest of 1.5 m or one fifth of wall height beyond the failure surface of 45 + ϕ/2. The lengths of anchors reduce linearly along the wall height. With the increase in the pile embedded depth, the amount of lateral displacement and also the rotation of the end of the pile decreases. According to the FHWA manual, the embedded depth of the pile is proposed in the range of 0.15 to 0.25 wall height. In this study, the largest value, *i.e.*, 0.25*H* was considered. In the numerical model, length of the front wall is equal to the wall height. Also, the distance from the bottom of the excavation to the bottom boundary of the model is equal to the wall height. The length of the soil behind the wall is 38 and 51 m for the wall height of 12 and 24 m, respectively. The type of input elements and meshing are consistent with the verification step. In Plaxis 3D calculation section, surcharge is used after applying the preliminary conditions of ground such as boundary and soil application and before pile activation. It is assumed in this step that the displacements become zero. Figure 4 shows a general view of the model including surcharge location, pile position, and the way to apply prestressing force.

After modeling, the Plaxis 3D output is drawn to achieve stress distribution. The graph is related to the pressure distribution imposed on the wall as shown by Fig. 5. The figure provides the stress distribution for the model with the height of 12 m, the distance between piles of 3 m, and the surcharge of 50 kN/m^2, and soil type 1. The distribution diagram for the horizontal pressure of soil at any height is achieved as shown by Fig. 6 using the pressure distribution imposed on the wall. By calculating the area below the horizontal pressure diagram, pressure distribution diagram is achieved along the wall height. The area below the diagram in wall length unit indicates the pressure on the soldier pile at that height. Meanwhile, the area below the horizontal pressure diagram regardless of stress concentration at pile location presents the pressure on lagging.

The numerical models were analysed using an cohesionless and surcharge-free soil to compare the results of numerical modeling using the apparent pressure graphs of Terzaghi and Peck (1967) and Tschebotarioff (1951) with sandy or clayey soil and no surcharge. To compare the results of the numerical modeling using the analytical relations proposed by Spencer *et al*. (1986), Perko and Boulden (2008), and Bing-Xiong *et al*. (2013), the analyses are performed respectively on the models with cohesionless and surcharge-free, cohesionless with surcharge of 50 kPa surcharge, and with cohesion and surcharge-free soils. The examinations are carried out for soil type 1 and type 2 with the pile distance of 3 m at two heights of 12 and 24 m.

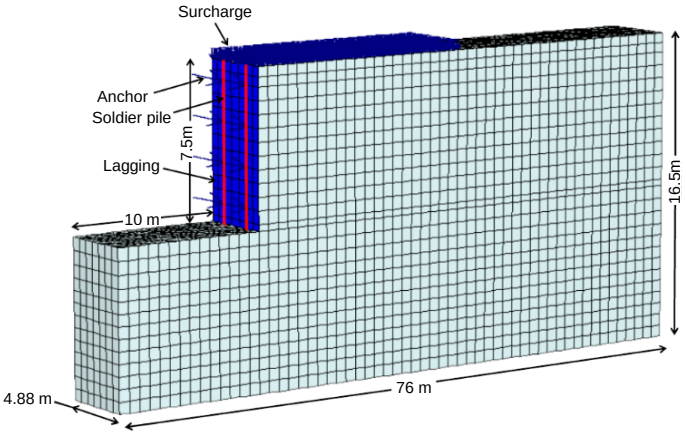

Fig. 4 General view of finite element model in Plaxis 3D Foundation

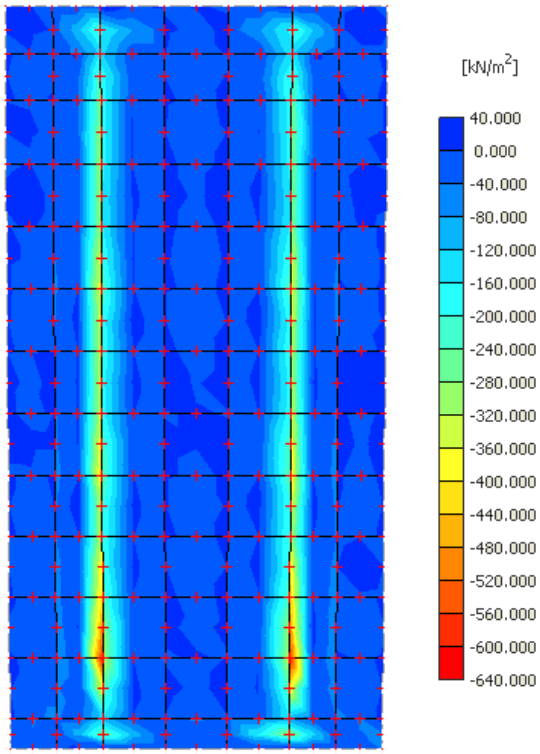

Fig. 5 Results of numerical modeling for normal pressure behind a 12 m high wall

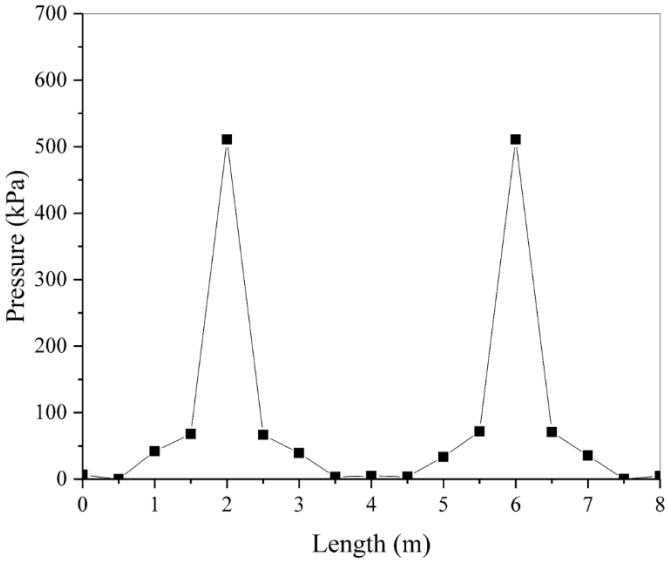

Fig. 6 Soil pressure distribution along horizon in the location of anchor at height of 10 m

4. RESULTS AND DISCUSSION

4.1 Soil Pressure on Soldier Pile

Figures 7 to 10 examine the diagrams related to the changes of pressure on the pile at wall height due to the change of soil type, amount of surcharge, wall height, and distance of piles. It should be noted that the values presented in the graphs include the amount of soil pressure on the length unit of wall and the pressure values should be multiplied by the horizontal distance of the piles.

Figure 7 compares the pressure imposed on the pile for type 1 and type 2 soils. The diagram shows the effect of type of soil on a wall with the height of 12 m, a pile with the centre-to-centre distance of 2 m, and the surcharge of 50 kPa. It shows that the pressure in type 2 soil has increased considerably. This is due to the reduction of cohesion from 30 kPa in soil type 1 to 10 kPa in soil type 2 and the reduction of soil friction angle from 36° in soil type 1 to 32° in soil type 2.

Figure 8 shows the effect of the distance of piles on the pressure imposed on the pile. The graph considered distances of 2, 3, and 4 m in the examination of the pressure imposed on the pile. As shown by the graph of Fig. 8, the pressure imposed on the length unit of the wall doesn't change by changing the distance of the piles; in other words, the force imposed on the piles is directly in proportion to the distance of piles.

Figure 9 examines the effect of surcharge. The proposed diagram has been prepared for 50, 100, and 150 kPa surcharges and a wall with the height of 12 m. Based on the diagram of Fig. 9, the surcharge has a direct effect on the pressure imposed on the pile. What is clear is that the graphs have a rising and increasing trend with the surcharge increasing from 50 to 100 and 150 kPa. Pressure becomes 1.5 to 2 times bigger with the surcharge increasing from 50 to 100 kPa.

Figure 10 shows the effect of wall height for soil type 1, the distance of 2 m, and the surcharge of 50 kPa. The increase of wall height from 12 to 24 m in Fig. 10 indicates the increasing trend of pressure applied to the pile. The pressure at the height of 24 m is almost 2 times bigger than the one at the height of 12 m.

Figure 11 compares the results obtained from the modeling using the graphs proposed by Terzaghi and Peck (1967) and Tschebotarioff (1951). The comparison is made while soil cohesion and surcharge are zero. In these conditions, the values obtained by Plaxis 3D are compared with the graphs proposed for sandy soil. The comparison was made for two types of soils, the wall height of 12 m, and the centre-to-centre distance of 3 m. As shown by the graph in Fig. 11, the pressure obtained from the relation proposed by Terzaghi and Peck (1967) is the lowest; Plaxis 3D values are more consistent with the values proposed by Tschebotarioff (1951). In the Plaxis 3D graphs, the breaking point of the diagram is at the beginning and at the end of the anchor location.

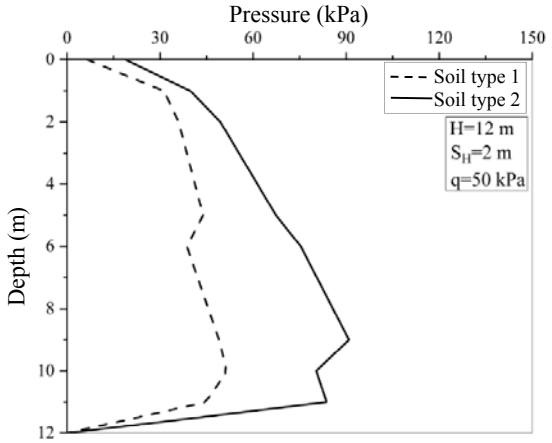

Fig. 7 Effect of soil type on pressure imposed on soldier pile

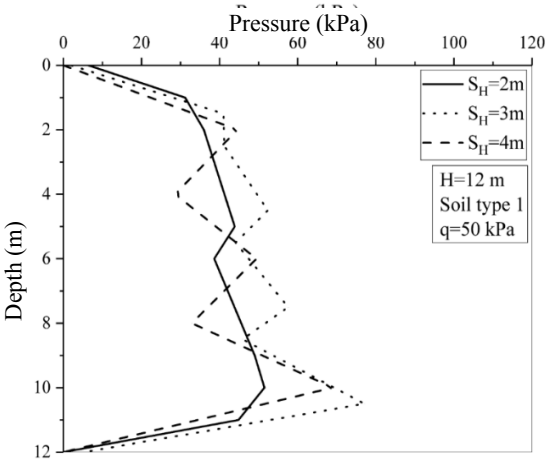

Fig. 8 Effect of piles spacing on pressure imposed on soldier pile

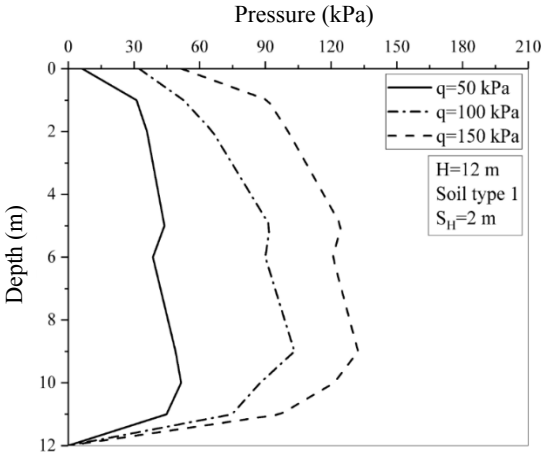

Fig. 9 Effect of surcharge on pressure imposed on soldier pile

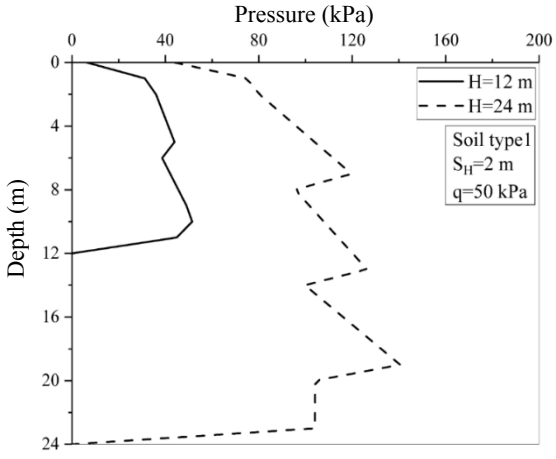

Fig. 10 Effect of wall height on pressure imposed on soldier pile

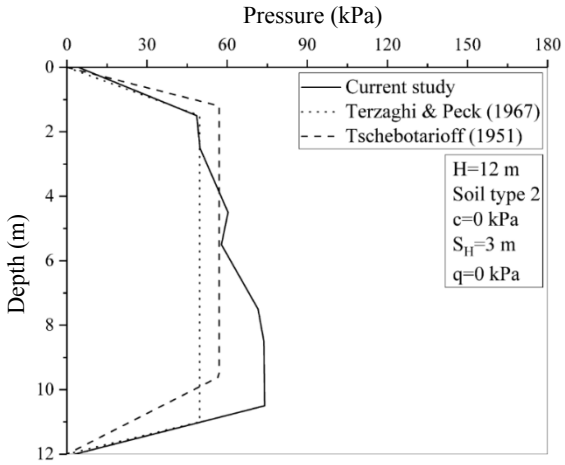

Fig. 11 Comparison of modeling results and available relations for pressure imposed on soldier pile

4.2 Soil Pressure on Laggings

Figures 12 to 15 show the diagrams related to pressure variation on lagging at the wall height due to the changes in type of soil, surcharge, height of wall, and distance of piles. Note that the values proposed by the graphs include the average pressure on lagging along the horizon between two soldier piles.

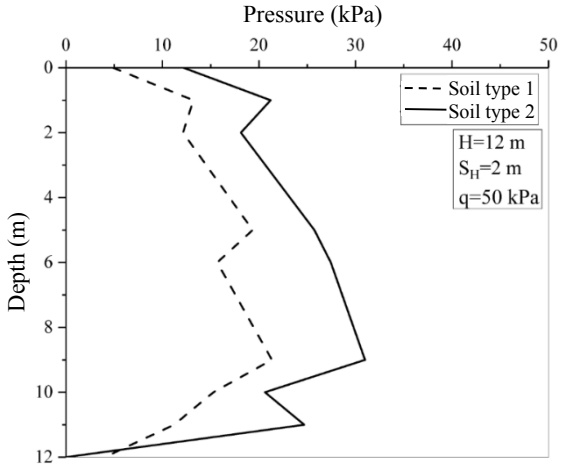

Fig. 12 Effect of soil type on pressure imposed on lagging

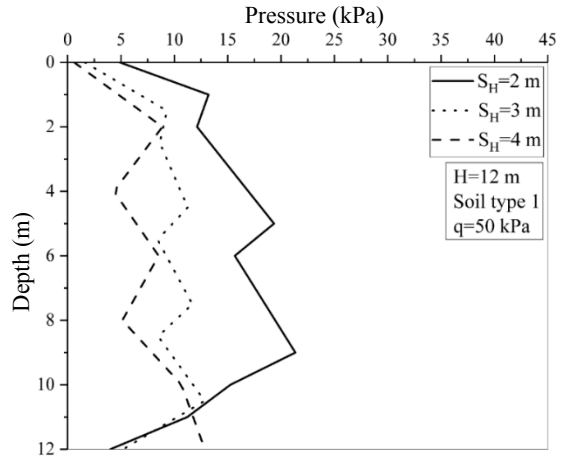

Fig. 13 Effect of piles spacing on pressure imposed on lagging

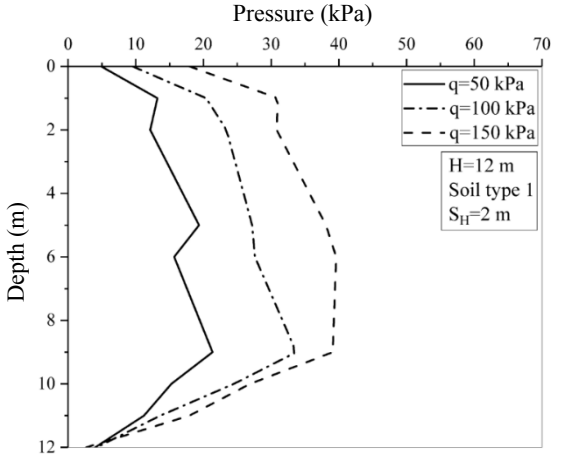

Fig. 14 Effect of surcharge on pressure imposed on lagging

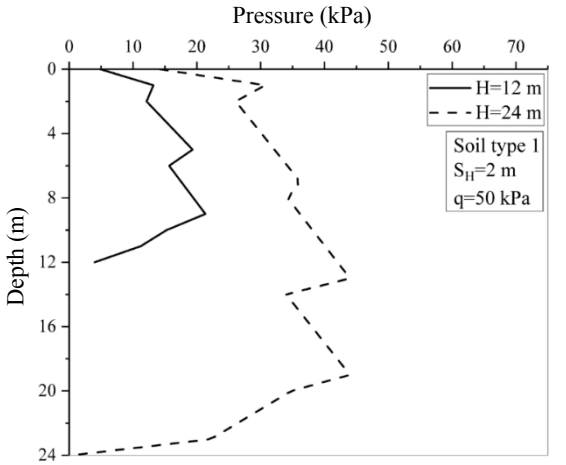

Fig. 15 Effect of wall height on pressure imposed on lagging

The effect of soil type is shown by Fig. 12. The graph compares soil type 1 and soil type 2 for the wall with the height of 12 m, the distance of 2 m, and the surcharge of 50 kPa. The graph shows the rate of pressure increase caused by the reduction of friction angle and soil cohesion. The relations show the pattern of pressure increase with the friction angle and soil cohesion decreasing.

The graph of Fig. 13 examines the effect of the distance between the piles on the pressure on lagging. As the graph shows, the pressure on the laggings in the unit of wall length reduces relatively with the distance between the piles increasing.

Figure 14 shows the effect of surcharge on the method of pressure distribution on the laggings. The comparisons were made for the wall height of 12 m, the centre-to-centre distance of 2 m, and soil type 1. The study surcharges were 50, 100, and 150 kPa. The trend of pressure changes in Fig. 12 is incremental. In fact, the pressure imposed on the wall with the surcharge increase from 50 to 100, and 150 kPa increases directly.

Figure 15 shows the effect of wall height on the behavior of the anchorage system and the way of pressure changes on the laggings. This figure discusses the effect of pressure on the lagging for the wall height of 12 and 24 m for a model with soil type 1, the centre-to-centre distance of 2 m, and the surcharge of 50 kPa. The pressure at the height of 24 m is almost 2 times bigger than the height of 12 m.

Figures 16 to 18 compare the modeling results and the values achieved from different analytical relations. The modeling results including soil type 2 with no cohesion, the center-to-center distance of 3 m, the wall heights of 12 and 24 m with no surcharge were compared with the analytical relations presented by Spencer *et al*. (1986), Perko and Boulden (2008),

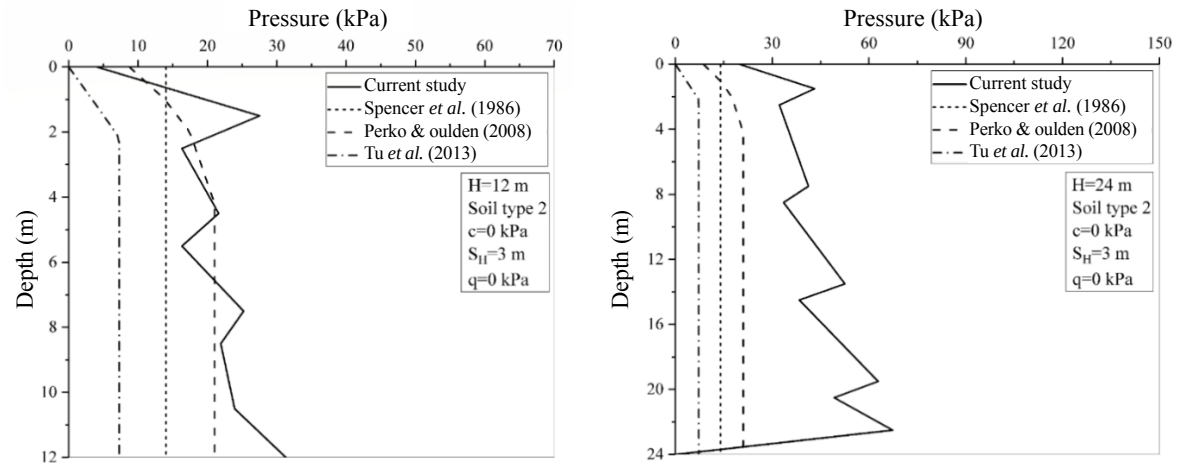

(a) Wall height = 12 m (b) Wall height = 24 m

Fig. 16 Comparison of modeling results and available relations for pressure imposed on lagging (soil type 2 without cohesion, without surcharge)

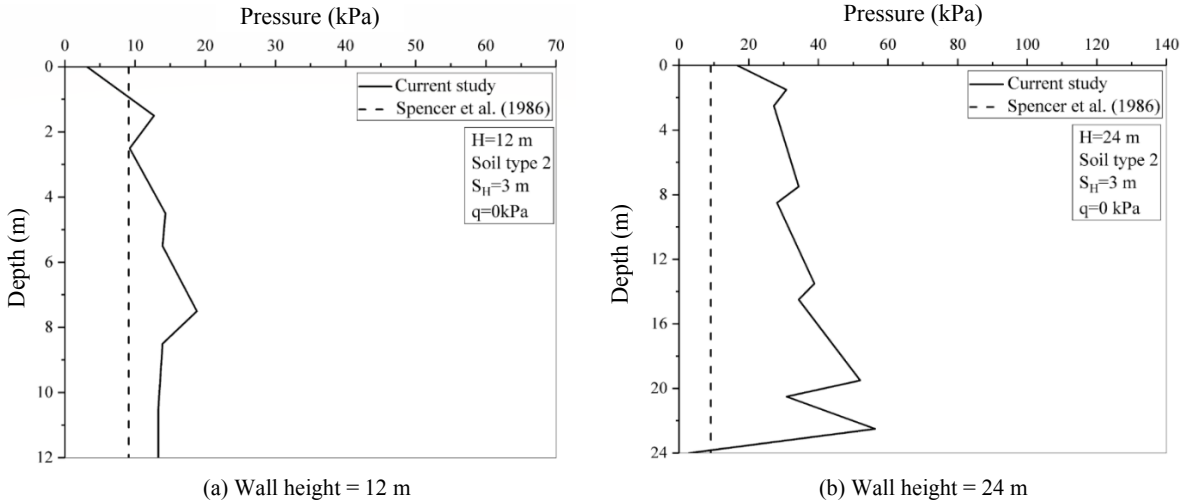

(a) Wall height = 12 m (b) Wall height = 24 m

Fig. 17 Comparison of modeling results and available relations for pressure imposed on lagging (soil type 2 without surcharge)

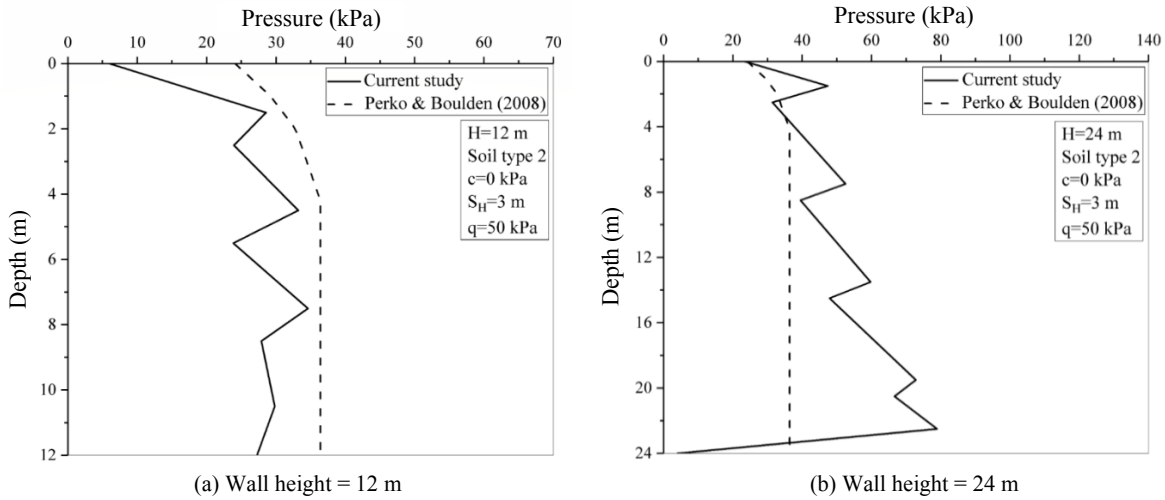

(a) Wall height = 12 m (b) Wall height = 24 m

Fig. 18 Comparison of modeling results and available relations for pressure imposed on lagging (soil type 2 without cohesion, with surcharge)

and Bing-Xiong *et al*. (2013) as per Fig. 16. It shows that for the identical values, the values obtained from Bing-Xiong *et al*. (2013) are minimal. This relation is slightly consistent with the numerical modeling values. The relation proposed by Perko and Boulden (2008) has the highest consistency with the research results. As shown by Figure 16(b), the difference between the values obtained from the modeling and the analytical relations become bigger at the height of 24 m. This is due to overlooking the effect of wall height on the pressure imposed on lagging. The modeling results were compared with the relation proposed by Spencer *et al*. (1986) as shown by Fig. 17. The modeling carried out in this concern includes soil type 2 with cohesion and the center-to-center distance of 3 m at two heights of 12 and 24 m with no surcharge. Figure 18 made a comparison between soil type 2 with no cohesion at two heights of 12 and 24 m for the surcharge of 50 kPa with the analytical relation proposed by Perko and Boulden (2008). In Figures 16, 17, and 18, the values proposed by the relations are consistent properly with the research modeling results for the depth of 12 m. Overlooking of the effect of wall height in the relations led to the inconsistency of numerical modeling results and the values for analytical relations at the height of 24 m.

5. THE PROPOSED RELATION FOR THE PRESSURE ON THE PILE AND LAGGING

Through examining the graphs obtained from the parametric analysis and studying the pattern of pressure change imposed on the pile and lagging, some graphs are presented for the pressure on the pile and lagging, which encompass all the effective parameters. The proposed diagram for the pressure on the soldier pile is as shown by Fig. 19. The pressure on the ground equals P_0. The stress on the ground is only affected by surcharge and cohesion and soil weight has no effect on it. Pressure is fixed and equal to P_1 from the first anchor to the last anchor. The pressure reduces and reaches zero from the location of the last anchor to the bottom of wall. The pressure values imposed on the pile is obtained from Eq. (2). On the sandy soil with no surcharge, the pressure obtained using the proposed relation is 30 percent higher than the one obtained from Terzaghi and Peck's relation. The conclusion indicates that the relation proposed by Terzaghi and Peck's can be reliable in the opposite direction.

The pressure distribution imposed on lagging has been proposed as shown by Fig. 20. The graph is made of two sections. A pressure equal to P_{0L}, which is a function of the surcharge, is imposed on laggings on the ground. From the location of the first anchor to the bottom of wall, pressure is fixed. Based on the results for parametric analyses, the pressure on the pile is almost 5 times higher than the stress imposed on lagging. The proposed equation in Eq. (3) indicates the pressure on lagging. The proposed equations are preliminary relations and various experimental and numerical studies should be done to better grasp the essence of the topic and develop comprehensive equations which can be used in various conditions.

The pressure values imposed on the pile:

$$P_0 = K_a\, q \qquad \text{for } h = 0 \tag{2a}$$

$$P_1 = \frac{0.75K_a\, H^2}{H - h_1 - h_3} - 2\sqrt{K_a}\, c + 1.7K_a\, q \quad \text{for } h_1 < h \le h_1 + h_2 \tag{2b}$$

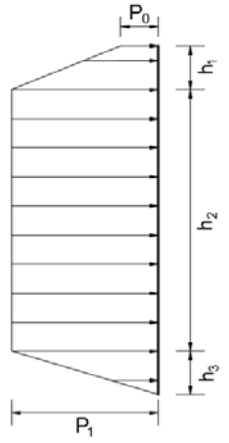

Fig. 19 Proposed diagram for pressure imposed on soldier pile

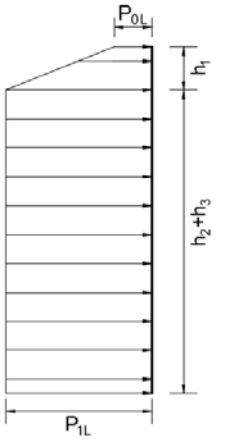

Fig. 20 Proposed diagram for pressure imposed on lagging

The pressure values imposed on the lagging:

$$P_{0L} = 0.2K_a\, q \qquad \text{for } h = 0 \tag{3a}$$

$$P_{1L} = 0.3K_a\, \gamma H - 0.4\sqrt{K_a}\, c + 0.3K_a\, q \quad \text{for } h > h_1 \tag{3b}$$

In the above relations:

h = Depth (m)
h_1 = The distance between the ground level and the location of the first anchor (m)
h_2 = $H - h_1 - h_3$
h_3 = The distance between the location of the last anchor to the bottom of the wall (m)
c = Soil cohesion (kPa)
q = Surcharge (kPa)
K_a = Lateral earth pressure coefficient
γ = Soil unit weight (kN/m^3)
H = Wall height (m)

The main enhancements of the proposed equations in comparison to the available relationships are:

- One of the advantages of the proposed equation is the simultaneous consideration of soil cohesion and friction angle.
- In the existing equations for the soil pressure on lagging, effect of wall height has not been taken into account, while according to the Table 12 of FHWA manual, the thickness

of lagging is defined for two heights of 0 ~ 8 and 8 ~ 18 m. This means that as the wall height increases, the soil pressure on lagging increases. As noticed, the wall height has been included in the proposed equations of this study.

- In the existing equations, the surcharge-induced pressure on the soldier pile and lagging is $K_a q$, while in the proposed relation it is equal to $1.7K_a q$ for soldier pile and $0.2K_a q$ for lagging.

6. CONCLUSIONS

The major research results are as follows:

1. The pressure on the soldier pile is considerably higher than the one imposed on the lagging, which emphasizes the occurrence of arching phenomenon. Results of analyses show that the effect of changing soil type, wall height, the distance between piles, and surcharge on the pressure imposed on the soldier pile is considerably higher than the one imposed on lagging.
2. Based on the parametric analysis, the pressure imposed on the anchored wall exceeded the values proposed in the apparent pressure diagrams. The average rate of pressure imposed on the pile is 1.3 times higher than the one presented by Terzaghi and Peck (1967).
3. The results indicate that the effect of surcharge on increasing the horizontal pressure of soil exceeds the classical relation. The coefficient in the relation is K_a and the calculation proves that the effect of surcharge is approximately 70% higher than this value.
4. Comparing the modeling results and the values achieved from different analytical relations indicates that overlooking of the effect of wall height in the analytical relations leads to incorrect estimation of soil pressure on lagging for the tall walls.

REFERENCES

Briaud, J. L. and Lim, Y. (1999). "Tieback walls in sand: numerical simulation and design implications." *Journal of Geotechnical and Geoenvironmental Engineering*, ASCE, **125**(2), 101-110. https://doi.org/10.1061/(ASCE)1090-0241(1999)125:2(101)

Brinkgreve, R.B.J. and Broere, W. (2004). *Plaxis 3D Foundation Reference Manual*.

Coulomb, C.A. (1776). "Essai sur une applcation des règles des maximis et minimis à quelques problèmes de statique, relatifs à l'architecture." Mémoires de mathématique & de physique présentés à l'Académie Royale des Sciences par divers savans & lûs dans ses assemblées, **7**, 343-382.

Ertugrul, N.A. (2013). *Effect of Soil Arching on Lateral Soil Pressures Acting upon Rigid Retaining Walls*. M.Sc. Thesis, The Graduate School of Natural and Applied Sciences of Middle East Technical University.

Fang, Y.S. and Ishibashi, I. (1986). "Static earth pressures with various wall movements." *Journal of Geotechnical Engineering*, ASCE, **112**(3), 317-333. https://doi.org/10.1061/(ASCE)0733-9410(1986)112:3(317)

Geol, S. and Patra, N.R. (2008). "Effect of arching on active earth pressure for rigid retaining walls considering translation mode." *International Journal of Geomechanics*, ASCE, **8**(2), 123-133. https://doi.org/10.1061/(ASCE)1532-3641(2008)8:2(123)

Handy, R.L. (1985). "The arch in soil arching." *Journal of Geotechnical Engineering*, ASCE, **111**(3), 302-318. https://doi.org/10.1061/(ASCE)0733-9410(1985)111:3(302)

Harrop-Williams, K.O. (1989). "Geostatic wall pressures." *Journal of Geotechnical Engineering*, ASCE, **115**(9), 1321-1325. https://doi.org/10.1061/(ASCE)0733-9410(1989)115:9(1321)

Hosseinian, S. and Cheraghi Seifabad, M. (2013). "Optimization the distance between piles in supporting structure using soil arching effect." *Journal of Civil Engineering and Urbanism*, **3**(6), 386-391.

Li, C.-F., Ye, X.-M., and Li, Y.-W. (2011). "Study of earth pressure of prestressed anchor pile considering soil arching." *Rock and Soil Mechanics*, **32**(6), 1683-1689.

Nadukuru, S.S. and Michalowski, R.L. (2012). "Arching in distribution of active load on retaining walls." *Journal of Geotechnical and Geoenvironmental Engineering*, ASCE, **138**(5), 575-584. https://doi.org/10.1061/(ASCE)GT.1943-5606.0000617

Paik, K.H. and Salgado, R. (2003). "Estimation of active earth pressure against rigid retaining walls considering arching effects." *Geotechnique*, **53**(7), 643-653. https://doi.org/10.1680/geot.2003.53.7.643

Perko, H. and Boulden, J. (2008). "Lateral earth pressure in soldier pile wall systems." *DFI Journal*, **2**(1), 46-54. https://doi.org/10.1179/dfi.2008.006

Sabatini, P.J., Pass, D.G., and Bachus, R.C. (1999). *FHWA-Geotechnical Engineering Circular No.4: Ground Anchors and Anchored Systems*. Federal Highway Administration, Report No. FHWA-IF-99-015.

Rashidi, F. and Shahir, H. (2017). "Numerical investigation of anchored soldier pile wall performance in the presence of surcharge." *International Journal of Geotechnical Engineering*. https://doi.org/10.1080/19386362.2017.1329258

Song, Y.S. and Hong, W.P. (2008). "Earth pressure diagram and field measurement of an anchored retention wall on a cut slope." *Landslides*, **5**(2), 203-211. https://doi.org/10.1007/s10346-007-0098-8

Spencer, White, and Prentis, Inc. (1986). "Lagging design." Sample calculations provided by Tom Tuozzolo, Moretrench Geotec, Rockaway, NJ (unpublished).

Terzaghi, K. (1943). *Theoretical Soil Mechanics*. John Wiley & Sons, Inc., New York, N.Y. https://doi.org/10.1002/ 9780470172766

Terzaghi, K. and Peck, R.G. (1967). *Soil Mechanics in Engineering Practice*. John Wiley & Sons, Inc., New York, N.Y.

Tsagareli, Z.V. (1965). "Experimental investigation of the pressure of a loose medium on retaining walls with a vertical back face and horizontal backfill surface." *Soil Mechanics and Foundation Engineering*, **2**(4), 197-200. https://doi.org/10.1007/BF01706095

Tschebotarioff, G.P. (1951). *Soil Mechanics, Foundation, and Earth Structures*. Mcgraw-Hill Book Company, Inc.

Tu, B.-X., Jia, J.-Q., Wang, H.-T., Cai, Y., and Yu, J. (2013). "Earth pressure on shotcrete of flexible retaining method with prestressed anchor." *Rock and Soil Mechanics*, **34**(12), 3567-3572.

Vermeer, P., Punlor, A., and Ruse, N. (2001). "Arching effect behind a soldier pile wall." *Computers and Geotechnics*, **28**(6-7), 379-396. https://doi.org/10.1016/S0266-352X(01)00010-6